Out-of-centre distortions around an octahedrally coordinated Ti4+ in BaTiO3

Manuel Gaudon

Out-of-centre distortions around an octahedrally coordinated Ti^{4+} in $BaTiO_3$

*Manuel Gaudon**

CNRS, Univ. Bordeaux, ICMCB, 33600 Pessac, France.

*corresponding author, ICMCB/CNRS, 87 avenue du Dr. Albert Schweitzer, F-33608 Pessac Cedex, France - email: gaudon@icmcb-bordeaux.cnrs.fr

Graphical Abstract

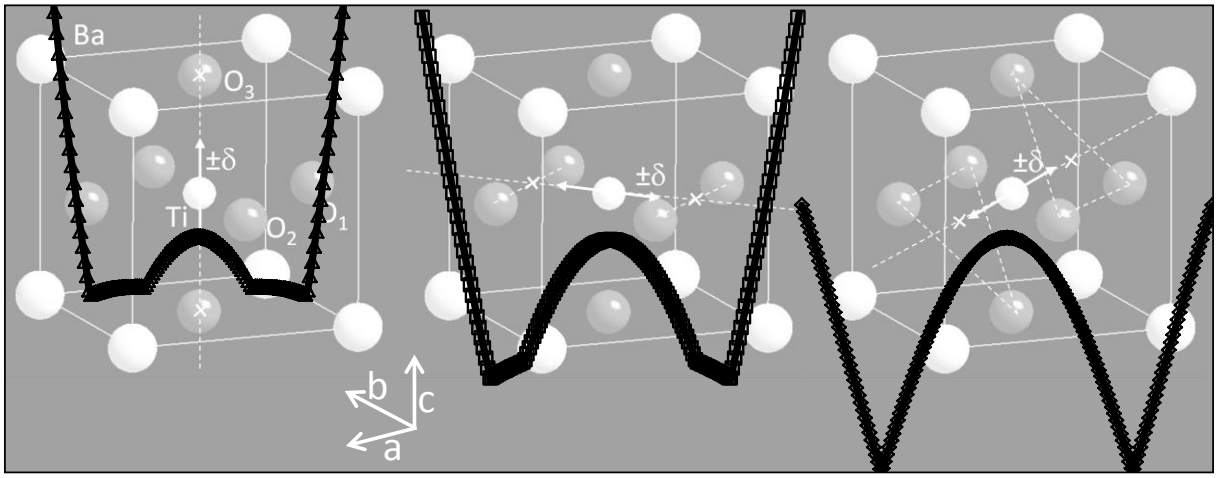

Out-of-centre distortions around an octahedrally coordinated Ti^{4+} in $BaTiO_3$

*Manuel Gaudon**

CNRS, Univ. Bordeaux, ICMCB, 33600 Pessac, France.

*corresponding author, ICMCB/CNRS, 87 avenue du Dr. Albert Schweitzer, F-33608 Pessac Cedex, France - email: gaudon@icmcb-bordeaux.cnrs.fr

Highlights

- Prediction of the Ti^{4+} position in the $BaTiO_3$ octahedral sites
- Prediction of the cubic-tetragonal-orthorhombic-rhomboedral phase transitions sequence
- Impact of the cell distortion on the Ti^{4+} position

Out-of-centre distortions around an octahedrally coordinated Ti^{4+} in $BaTiO_3$

*Manuel Gaudon**

CNRS, Univ. Bordeaux, ICMCB, 33600 Pessac, France.

*corresponding author, ICMCB/CNRS, 87 avenue du Dr. Albert Schweitzer, F-33608 Pessac Cedex, France - email: gaudon@icmcb-bordeaux.cnrs.fr

Abstract

The prototypical ferroelectric system $BaTiO_3$ is an oxide with a perovskite-type structure that exhibits a textbook example of multiple phase transitions associated with an out-of-centre distortion of the octahedral Ti^{4+} cations. This research combines the double-well potentials model and the bond valence model, to provide an explanation for the cubic–tetragonal–orthorhombic–rhombohedric phase transition sequence. It is shown that to consider the atomic displacements can only occur in the strict respect of their valence, which is calculated with the bond valence model, is sufficient to lead to the clear prediction of the whole transition sequence.

Keywords: Phase transitions; perovskite; bond valence; thermodynamics.

Introduction

Numerous investigations of the $BaTiO_3$ transitions have been proposed in the literature. 20 years ago, the general consensus that both short-range ionic attractions and long-range ordering must be considered, has definitely emerged [1]. Recently, first-principles density functional theory integrating molecular dynamics have led to a better prediction of the phase transitions parameters [2-6]. This is interesting to note that latest reviews, essentially under the impulse of Polinger and Bersuker, point out essentially that the spontaneous polarization

is triggered by local vibronic interactions as pseudo Jahn-Teller effect (named as "second order Jahn-Teller effect, for other authors) [7-11]. It will be seen that in a quite similar manner that what is proposed in this paper, the Jahn-teller interactions result in a peculiar adiabatic potential energy surface (APES) which has eight trigonal [111] type minima, twelve [110] type saddle points between them, six higher in energy [100] type saddle points at the top of the barrier connecting four minima, and a maximum at the cubic symmetry. Nevertheless, it stills interesting to propose simplest models pointing out clearly the driving force.

To provide a new avenue for investigating the $BaTiO_3$ phase transition sequence—cubic–tetragonal–orthorhombic–rhombohedric—that occurs with decreasing temperature, we combined the approaches based on the bond valence model [12,13] and the coupled double-well potentials initially proposed by Aubry [14,15], which is widely referenced throughout the literature to describe the second-order phase transitions [16-20].

Results and Discusssion

In the bond valence model, each bond is characterised by a bond valence (s) equal to the atomic valence contributed by each terminal atom that is correlated with the bond length (r) by the following relationship [21]:

$$s = \exp(r_0 - r) / B \qquad \text{equation (1)}$$

in which r_0 and B are parameters that have been tabulated: for the Ti-O bond, r_0 = 1.81 Å, and B = 0.37 in oxides.

Around an atom, the sum of the bond valences is equal to the atomic valence (V). The ideal valences for titanium and oxygen are obviously $V(Ti^{4+})= 4$ and $V(O^{2-})= 2$. A valence sum rule was also proposed by Brown and indicates that the ionic crystals are more stable than the atomic valences near the ideal conditions. In $BaTiO_3$, the Ba-O bonds are too long and the Ti-O bonds too short for an ideal fit (tolerance factor far from the unity). Consequently, for the

perovskite-type structure to exist, the Ti-O bonds must be stretched so that the sum of their bond valences, which can be calculated using equation (1), becomes significantly lower 4.0. As a result of this structural inconsistency in the $BaTiO_3$ perovskite phase, the environment of the Ti^{4+} cation will tend to distort to better satisfy the Ti^{4+} valence sum rule. At the expense of equation (1), the out-of-centre shift of the Ti^{4+} in its coordination sphere allows its atomic valence to increase. The decrease in one bond distance and the increase of the same magnitude in the opposite bond distance results in a net valence increase. The above proposition was made by Kunz and Brown [13] and was herein considered a good starting point for understanding the driving force of the various phase transitions in $BaTiO_3$ that occur at low temperatures.

The coupled double-well potentials model is a useful tool for studying phase transitions. The model contains an array of atoms with one atom in each unit cell and atoms that are linked by harmonic forces (which can be represented as springs). These harmonic forces provide a cooperative interaction at the origin of the long-range ordering. Each atom experiences a local double-well potential that provides the driving force for the phase transition such as the potential experienced by the Ti^{4+} in $BaTiO_3$. In its simplest version, this model provides a scalar (one-dimensional) displacement of each atom (δ), and the local double-well potential [1,16] can be represented as follows:

$$W(\delta) = -\tfrac{1}{2}\times K\times\delta^2 + \tfrac{1}{4}\times K'\times\delta^4 \qquad \text{equation (2)}$$

in which the parameters K and K' are positive constants.

Two important quantities can be distinguished: (i) the depth of the potential well (W_0) and (ii) the interaction energy between two neighbouring atoms, i.e., the spring force (J). This model can easily be generalised to higher dimensions to better fit a real 3D crystal network.

Our research serves as a continuation of that by Kunz and Brown to propose an empirical double-well potential equation using the established bond valence model. Our idea that seems

trivial but is actually important is the potential that an octahedrally coordinated titanium in $BaTiO_3$ can be assumed on first approximation to be proportional to the modulus of the deviation between the calculated valence of the titanium and its ideal valence (4).

The calculated valence of titanium can be extracted as a function of the Ti position in the cell using the out-of-centre distortion, δ, according equation (2). Therefore, the calculation of the double-well potential versus the displacement amplitude was calculated in the three distortive modes: [001] for the tetrahedral distortion, [110] for the orthorhombic distortion and [111] for the rhombohedral distortion. Our description is based on three distinctive distortion modes unlike the model proposed by Comes et al. [22] in which the various phases are believed to derive from order–disorder transitions from a rhombohedral mode. The cell was fixed as a pseudo-cubic cell with the a_0 parameter equal to 4.02 Å. Only Ti^{4+} was considered to have an out-of-centre distortion, i.e., the Ba^{2+} and O^{2-} ions were considered fixed.

(i) In the tetrahedral mode

$$W(\mathrm{Ti}) = \mathrm{modulus}\ \{ 4 - 4.\exp[[r_0 - (a_0/2)^2 + \delta^2]^{0.5} / B] - \exp[[r_0 - a_0/2 - \delta] / B] - \exp[[r_0 - a_0/2 + \delta] / B] \} \quad \text{equation (3)}$$

(ii) In the orthorhombic mode

$$W(\mathrm{Ti}) = \mathrm{modulus}\ \{ 4 - 2.\exp\mathbf{[}[r_0 - \mathbf{(}a_0/2/\sqrt{2} + \delta\mathbf{)}^2 + \mathbf{(}a_0/2/\sqrt{2}\mathbf{)}^2]^{0.5} / B\mathbf{]} - 2.\exp\mathbf{[}[r_0 - \mathbf{(}a_0/2/\sqrt{2} - \delta\mathbf{)}^2 + \mathbf{(}a_0/2/\sqrt{2}\mathbf{)}^2]^{0.5} / B\mathbf{]} - 2.\exp\mathbf{[}[r_0 - \mathbf{(}a_0/2\mathbf{)}^2 + \delta^2]^{0.5} / B\mathbf{]}\ \} \quad \text{equation (4)}$$

(iii) In the rhombohedral mode

$$W(\mathrm{Ti}) = \mathrm{modulus}\ \{ 4 - 3.\exp\mathbf{[}[r_0 - \mathbf{(}a_0/2/\sqrt{3} + \delta\mathbf{)}^2 + \mathbf{(}a_0.\sqrt{2}/2/\sqrt{3}\mathbf{)}^2]^{0.5} / B\mathbf{]} - 3.\exp\mathbf{[}[r_0 - \mathbf{(}a_0/2/\sqrt{3} - \delta\mathbf{)}^2 + \mathbf{(}a_0.\sqrt{2}/2/\sqrt{3}\mathbf{)}^2]^{0.5} / B\mathbf{]}\ \} \quad \text{equation (5)}$$

Figure 1(a) provides the calculated double-well potential W(Ti) versus the displacement δ for the three distortion modes. The W_0 values were obtained for roughly similar displacements in the three modes. Thus, the origin of the double-well potential associated with the out-of-centre distortions is already explained by taking into account only the fit of the titanium bond

valences in the perovskite and the ideal Ti^{4+} valence. Nevertheless, the reason that the three distortion modes all occur with decreasing temperature remains an open question. In the second step, the double-well potential was calculated for the [TiO3] octahedral pattern as the sum of the W(Ti), $W(O_1)$, $W(O_2)$ and $W(O_3)$ moduli. The calculation of the W(O) was made with a rule similar to that for the W(Ti). The ideal partial valence that the oxygen anions must exchange with their two neighbouring Ti^{4+} cations is 4/3; the oxygen anions must also exchange an ideal valence of 2/3 with their four neighbouring Ba^{2+} cations. The double-well potential was established using a cooperative long-range ordering of the titanium cations to account for the three distortion modes. Hence, as an example, the W(O3) in the tetrahedral mode can be written as follows:

$$W(O3) = \text{modulus} \{ 4/3 - \exp[[r_0 - a_0/2 - \delta) / B] - \exp[[r_0 - a_0/2 + \delta) / B] \} \quad \text{equation (6)}$$

Figure 1(b) represents the double-well potentials obtained in the three modes for the [TiO3] pattern. The three modes present different double-well potential depths. Classifying the double-well depth in increasing order, i.e., classifying the modes versus their driving force, a tetrahedral–orthorhombic–rhombohedral sequence is obtained. This sequence is strongly correlated to the experimental order observed for $BaTiO_3$ phases with decreasing temperature. However, the occurrence of the intermediate modes at intermediate temperatures remains unexplained, i.e., there is no a priori explanation as to why the direct transition from the cubic to rhombohedral phase fails to occur. The depth of the double-well potential for the tetrahedral and orthorhombic modes is never null due to a decoupling of the evolution versus the displacement between the oxygen anions and the titanium cation valences. In an opposite manner, the evolution of the [111] valence displacements between the central cation and the three oxygen corners in the rhombohedral mode are perfectly coupled. This behaviour is best illustrated by extracting the evolution of the $W(O_{tensor})$ (see Figure 2(a)). The term O_{tensor} represents the oxygen the most impacted by the Ti^{4+} out-of-centre distortion: the O3 in the

tetrahedral mode, the O1 (or O2) for the orthorhombic mode and the O1 (O2 or O3) for the rhombohedral mode. The O_{tensor} can also be considered the spring force between two successive Ti^{4+} ions. Until now, a perfect long-range ordering was only considered, i.e., a purely cooperative (or efficient ferroelectric ordering or "ferro-coupling"). In an opposite manner, the impact of an "antiferro-coupling" of two neighbouring Ti^{4+} ions can be discussed. As example, in the tetrahedral mode, the double-well potentials of the Ti^{4+} ions and the O1 and O2 remain unchanged in comparison with those in a cooperative ordering. In contrast, the valence of the O3 oxygen will be strongly affected because, in this case, two long ($a_0/2 + \delta$) or two short ($a_0/2 + \delta$) Ti-O distances could coexist around the oxygen tensor. In a ferro-coupled chain, the occurrence of an antiferro-coupled fault could automatically cause the creation of two frustrated oxygen tensors (one with two long Ti-O distances and one with two short Ti-O distances). Thus, the evolution of the $W(O_{tensor})$ versus the displacement δ for an antiferro-coupling can be calculated as follows:

$$W(O3) = \tfrac{1}{2}.\text{modulus}\ \{\ 4/3 - 2.\exp\mathbf{[}[r_0 - a_0/2 + \delta\mathbf{)} / B\mathbf{]}\ \} + \tfrac{1}{2}.\text{modulus}\ \{\ 4/3 - 2.\exp\mathbf{[}[r_0 - a_0/2 - \delta\mathbf{)} / B\mathbf{]}\ \} \qquad \text{equation (7)}$$

In Figure 2(b), the $W(O_{tensor})$ for the three modes is reported considering two half-spaces: the antiferro-coupled half-space is plotted on the left (negative displacements), and the ferro-coupled half-space is plotted on the right (positive displacements). The interaction between two successive Ti^{4+} ions via the O_{tensor} anion can be considered strongly linked to the $W(O_{tensor})$ potential in the antiferro-coupled half-space. As shown in Figure 2(b), the frustration created by an eventual exploration of the antiferro-coupled half-space grows according to the following sequence: rhombohedral–orthorhombic–tetrahedral, especially on the tensor atom. The interaction energy *J* at the origin of the long-range cooperative ordering can obviously follow the same sequence. One can consider the interaction energy *J* as a

function of the amplitude between the two half-space explorations (δ) on the $W(O_{tensor})$ on the double-well potential:

$$\boldsymbol{J(\delta) = K'' \times \left(\int_{-\delta}^{0} W(\mathbf{O_{tensor}}) d\delta - \int_{0}^{\delta} W(\mathbf{O_{tensor}}) d\delta \right)} \quad \text{equation (8)}$$

in which the parameter K'' is a positive constant. The energy function $J(\delta)$ versus δ is plotted for the three modes in Figure 3. The proportionality of J and T_C (the phase transition temperature) is provided in the literature [23,24]. The T_C sequence in increasing order is then : rhombohedral–orthorhombic–tetrahedral.

The calculations were made considering a pseudo-cubic cell; however, all distortion modes are associated with additional atomic displacements and a cell distortion. The W(TiO3) was once again calculated in a realistic tetragonal phase (with a_T = 3.995 Å and c_T = 4.035 Å) taking into account the apical atoms and the equatorial plane shift of the octahedron: considering the out-of-centre Ti^{4+} as equal to $+\delta$, an equivalent displacement of the apical oxygen ions occurs in the opposite direction (a displacement equal to $-\delta$), and a displacement of $-\delta/2$ occurs for the equatorial oxygen ions. These considerations were based on the crystal structure investigated by Kwei et al. [20]. The as-obtained results are compared to the previous results in a pseudo-cubic cell depicted in Figure 4(a). The δ displacement (0.16 Å) associated with W_0 is more realistic in the second case approaching the tetrahedral $BaTiO_3$ real positions but not yet equal to the experimental δ : 0.09 Å [25].

The thermal vibrations of the atoms around their average positions have to be taken into consideration. The impact of the thermal vibrations can be roughly simulated considering that for each average δ displacement at temperatures above 0 K, the W(TiO3) is equal to the integer of all W(TiO3) values obtained at 0 K around the same displacement with an integration amplitude equal to the thermal vibration. This calculation corresponds to a mathematical smoothing of the double-well potential with a chosen smoothing degree that corresponds to the thermal vibration. For tetrahedral mode as illustration, a thermal vibration

amplitude of 0.1 Å must be computed to reach a W_0 positioning at 0.09 Å with then a correct set of Ti-O distances, as shown in Figure 4(b). The equivalence of the thermal vibration amplitude (0.1 Å) and the out-of-centre displacement (phonon mode = 0.09 Å) explains the experimental difficulties in extracting accurate atomic positions from X-ray diffraction and why the extent of the order–disorder versus displacive character remains, from our knowledge, unsettled for the $BaTiO_3$ perovskite [26].

Conclusion

Using an accessible approach (based on the double-well potential models and the bond valence model), the inverse relationships between the sequences described by the double-well potential depths (driving force, crystal energy) and the interaction energies (phase transition temperature) calculated for the various distortion modes of the $BaTiO_3$, clearly indicate that decreasing temperatures cause a cubic–tetragonal–orthorhombic–rhombohedral phase transition sequence. The position of the double-well potentials were also shown to correspond to experimental value if the cell parameters are well computed. The choice was made here to discuss only about the $BaTiO_3$ textbook example, for which the lattice stresses due to structural incommensuration (tolerance factor far from the unity) very clearly predominates as the driving force of the ferroelectric behaviour. Nevertheless, the propose can be extended to other perovskite systems as $SrTiO_3$ for illustration, for which the Sr-O bonds still are too long in comparison with Ti-O ones. Notice that the lattice stresses are already decreased for $SrTiO_3$ in comparison with $BaTiO_3$ (as Sr^{2+} ions are smaller than Ba^{2+} ions), predicting a stabilization of the cubic phase to the detriment of the distorted polymorph systems. Another example is the $BaSnO_3$ compound for which the cubic phase is stable at low temperature since the Sn is larger than Ti. On the other side, some ABO_3 perovskite systems present opposite stresses due to B-O bonds too long in comparison with the A-O bonds. The model here used should so be

applied taking into consideration the A metal out-of-center distortion and/or octahedral tilts. Recently, we proposed an ab-initio calculation of the fluorine ions positions in Rb_2KInF_6 double perovskites (elpasolite systems) correlated to octahedral tilts from the same consideration than in this paper (strict respect of the valence law) but, by manipulating the atomic positioning of the F^- anions [27].

We insist on the fact that in this easy approach, largely comprehensive to the chemist community, the strict respect of their valence of all the elements of the structure is the only proposition (and parameter) to integer to lead to the clear prediction of the whole transition sequence.

Acknowledgements

I would like to thank Antoine Villesuzanne for discussions regarding the phase transitions in perovskite.

References

[1] M.T. Dove, Am. Mineralog. 82 (1997) 213.

[2] T. Nishimatsu, M. Iwamoto, Y. Kawazoe, U.V. Waghmare, Phys. Rev. B 82 (2010) 134106.

[3] T. Hashimoto, T. Nishimatsu, H. Mizuseki, Y. Kawazoe, A.Sasaki, Y. Ikeda, Jpn. J. Appl. Phys. 43 (2004) 6785.

[4] T. Nishimatsu, U. V. Waghmare, Y. Kawazoe, D. Vanderbilt, Phys. Rev. B 78 (2008) 104104.

[5] Z.G. Wu, R.E. Cohen, Phys. Rev. B 73 (2006) 235116.

[6] R. Wahl, D. Vogtenhuber, G. Kresse, Phys. Rev. B 78 (2008) 104116.

[7] I.B. Bersuker, I.B. Journal of Physics: Conference Series 428 (2013) 012028.

[8] V. Polinger, Journal of Physics: Conference Series 428 (2013) 012026.

[9] I.B. Bersuker, Chem. Rev. 113 (2013) 1351-1390.

[10] U. Öpik M.H.L. Pryce, Proc. R. Soc. London A (1957) 238.

[11] O.F. Schirmer, Ferroelectrics 303 (2004) 131.

[12] M. Kunz, I.D. Brown, J. Solid State Chem. 115 (1995) 385.

[13] I.D. Brown, The Chemical Bond in Inorganic Chemistry, first ed., Oxford University Press Inc., New York, 2002.

[14] S. Aubry, J. Chem. Phys. 62 (1975) 3217.

[15] S. Aubry, J. Chem. Phys. 64 (1976) 3392.

[16] R.E. Cohen, H. Krakauer, Phys. Rev. B 42 (1990) 6416.

[17] A.D. Bruce, Adv. Phys. 29 (1980) 11.

[18] R. Currat, Collection SFN 10 (2012) 563.

[19] J.A. Krumhasnl, J.R. Schrieffer, Phys. Rev. B 11 (1975) 3535.

[20] S. Tinte, M.G. Stachiotti, M. Sepliarsky, R.L. Migoni, C.O. Rodriguez, J. Phys.: Condens. Matter 11 (1999) 9679.

[21] I.D. Brown, D. Altermatt, Acta Crystallog. Sect. B 41 (1985) 244.

[22] R. Comès, M. Lambert, A. Guinier, Acta Crystallog. Sect. A 26 (1970) 244.

[23] A.D. Bruce, R.A. Cowley, Structural Phase Transitions, Taylor and Francis (Eds), London, 1981.

[24] S. Radescu, I. Extebarria, J.M. Perez-Mato, J. Phys.: Condens. Matter 7 (1995) 585.

[25] G.H. Kwei, A.C. Lawson, S.J.L Billinge, S.-W. Cheong, J. Phys. Chem. 97 (1993) 2368.

[26] J.-M. Kiat, G. Baldinozzi, M. Dunlop, C. Malibert, B. Dkhil, C. Ménoret, O. Masson, M.-T. Fernandez-Diaz, J. Phys.: Condes. Matter 12 (2000) 8411.

[27] L. Cornu, M. Gaudon, Ph. Veber, A. Villesuzanne, A. Garcia, V. Jubera, submitted to Chemistry: A European Journal (2014).

Figure captions

Figure 1: Double-well potentials around Ti^{4+} (i): (a) *W*(Ti) and (b) *W*(TiO3) double-well potentials versus the Ti^{4+} out-of-centre distortion (δ) along the [100], [110] and [111] axes.

Figure 2: Double-well potentials around Ti^{4+} (ii): *W*(O_{tensor}) double-well potentials versus the Ti^{4+} out-of-centre distortion (δ) along the [100] axis considering (a) long range ordering (ferro-coupled domain) and (b) the comparison between the antiferro-coupled and ferro-coupled half spaces.

Figure 3: Coupled force versus distortion: The coupled force $J(\delta)/K''$ versus the Ti^{4+} out-of-centre distortion (δ) along the [100] axis calculated as the difference between the double-well integers on each half-space up to δ.

Figure 4: Double-well potentials around Ti^{4+} (iii): (a) Comparison of the ferro-coupled *W*(TiO3) double-well potential along the [100] axis considering pseudo-cubic or real tetragonal cells. (b) A comparison of the ferro-coupled *W*(TiO3) double-well potential in the tetrahedral modes both considering and ignoring the thermal vibrations in addition to the soft phonon mode.

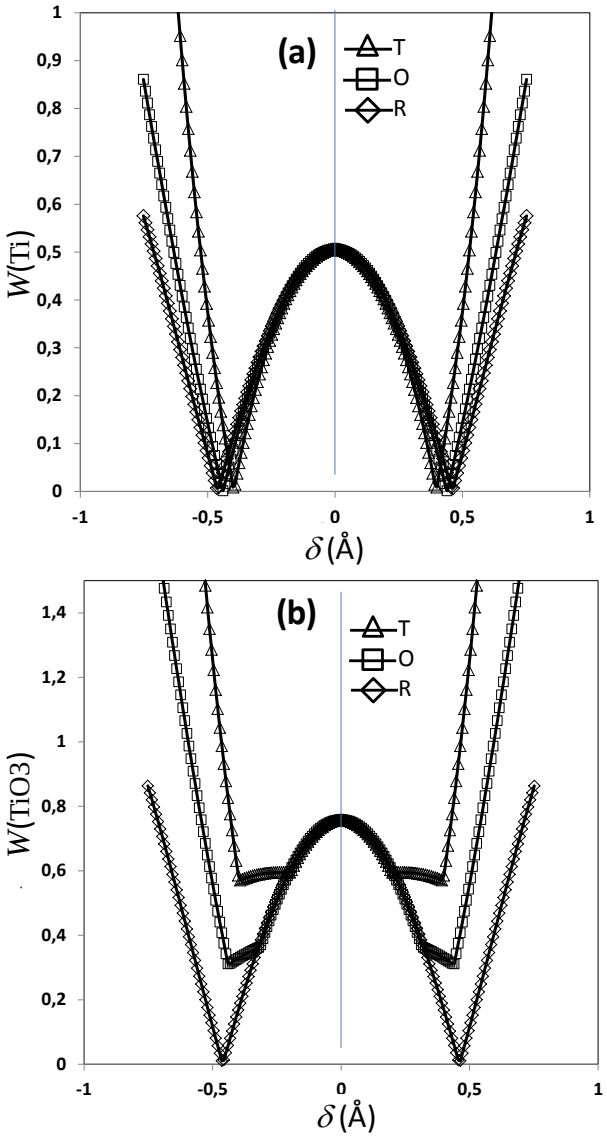

Figure 1

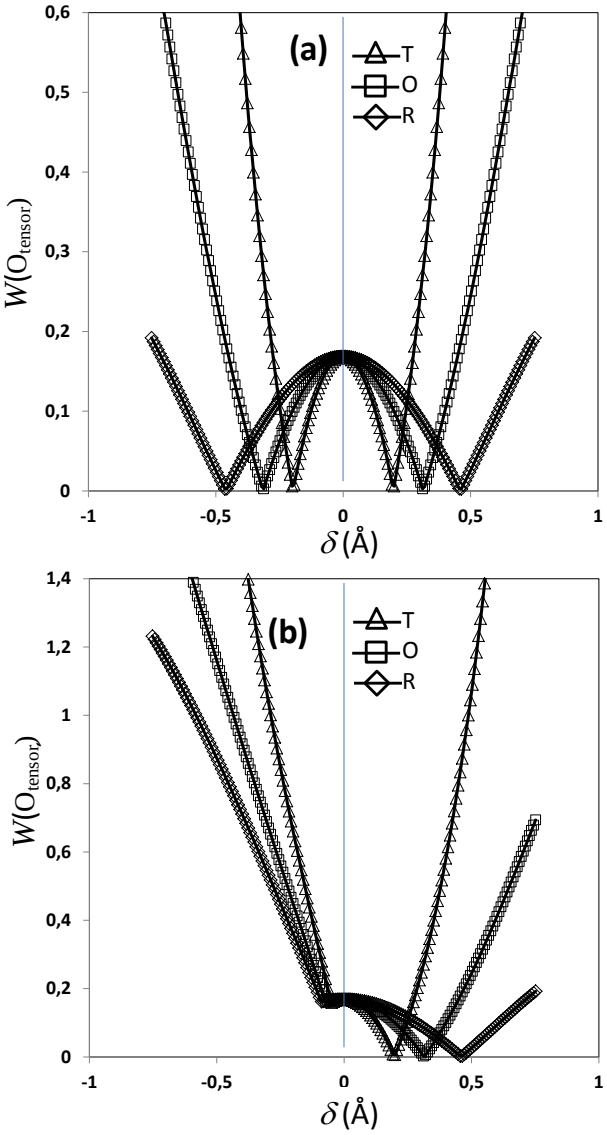

Figure 2

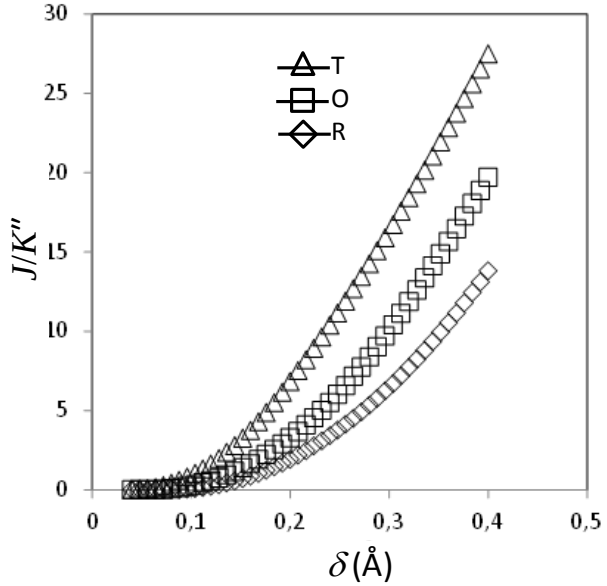

Figure 3

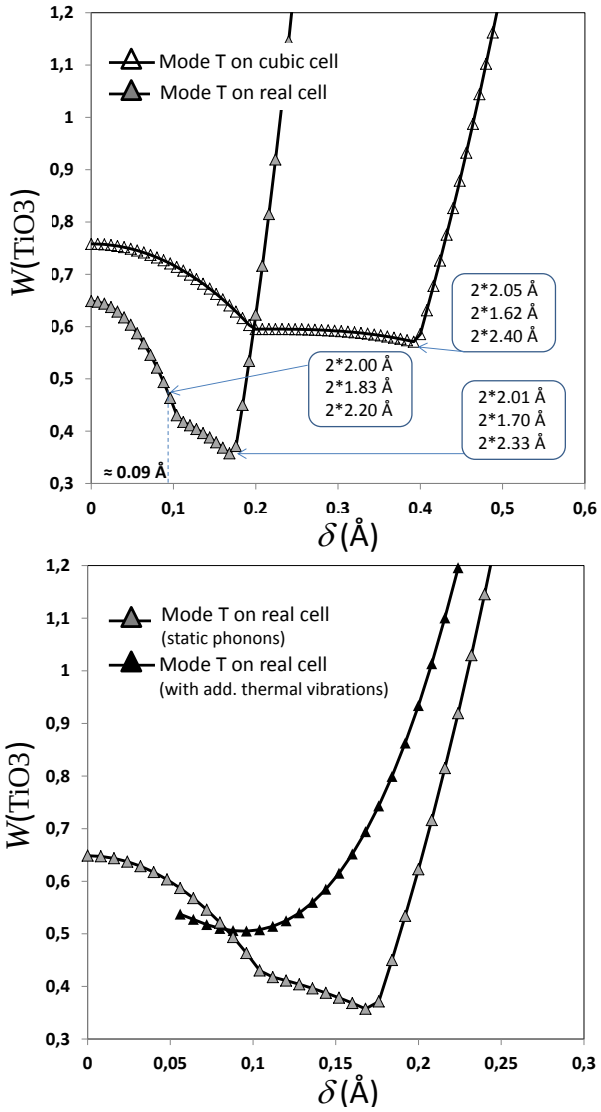
Mode T on cubic cell
Mode T on real cell
2*2.05 Å
2*1.62 Å
2*2.40 Å
2*2.00 Å
2*1.83 Å
2*2.20 Å
2*2.01 Å
2*1.70 Å
2*2.33 Å
≈ 0.09 Å
W(TiO3)
δ(Å)
Mode T on real cell
(static phonons)
Mode T on real cell
(with add. thermal vibrations)
W(TiO3)
δ(Å)

Figure 4